Compound imaging using Synthetic Aperture Sequential Beamformation

Jensen, Casper Bo; Jensen, Jonas; Hemmsen, Martin Christian; Hansen, Jens Munk; Jensen, Jørgen Arendt

Published in:
Proceedings of 2011 IEEE International Ultrasonics Symposium

Link to article, DOI:
10.1109/ULTSYM.2011.0565

Publication date:
2011

Document Version
Early version, also known as pre-print

Paper presented at the IEEE International Ultrasonics Symposium, Orlando Florida, 2011:

Compound imaging using Synthetic Aperture Sequential Beamformation

Casper Bo Jensen, Jonas Jensen, Martin Christian Hemmsen, Jens Munk Hansen and Jørgen Arendt Jensen

Center for Fast Ultrasound Imaging,
Biomedical Engineering group, Department of Electrical Engineering, Bldg. 349,
Technical University of Denmark, DK-2800 Kgs. Lyngby, Denmark

To be published in Proceedings of IEEE International Ultrasonics Symposium, Orlando Florida, 2011.

Compound imaging using Synthetic Aperture Sequential Beamformation

Casper Bo Jensen, Jonas Jensen, Martin Christian Hemmsen, Jens Munk Hansen and Jørgen Arendt Jensen
Center for Fast Ultrasound Imaging, Department of Electrical Engineering, Technical University of Denmark, Lyngby, Denmark

***Abstract*— Synthetic Aperture Sequential Beamforming (SASB) is a technique with low complexity and the ability to yield a more uniform lateral resolution with range. However, the presence of speckle artifacts in ultrasound images degrades the contrast. In conventional imaging speckle is reduced by using spatial compounding at the cost of a reduced frame rate. The objective is to apply spatial compounding to SASB and evaluate if the images have a reduced speckle appearance and thereby an improved image quality in terms of contrast compared to ordinary SASB.**

Using the simulation software Field II, RF data are acquired for a phantom with cysts at different sizes and scattering levels. 192 scanlines are recorded for five steering angles (0, ± 2, ± 4 degrees) using a 192 element linear array transducer. SASB is performed for each angle using a rectangular grid in the second stage beamformation. After envelope detection the five second stage images are added to form the compounded image. Using a ProFocus scanner and the 8804 linear array transducer (BK Medical, Herlev, Denmark) measurements of a phantom containing water filled cysts are obtained to validate the simulation results. The setup is the same as in the simulations and SASB second stage beamformation data are processed offline for each of the five angles. Contrast-to-noise ratio (CNR) and speckle-to-noise ratio (SNR) are extracted for the compounded image and the reference image (ordinary SASB).

CNR was calculated for the simulated cysts at depths of 40, 50, 60, 70 and 80 mm. On average the CNR was improved by 33.2% compared to the values obtained from the reference image. For regions of increasing depth SNR was on average increased by 9.3%. Results from the simulation were confirmed by calculations on the measured data. CNR of cysts at depths from 18 to 78 mm with a separation of 10 mm was on average improved by 45.9%. On average an improvement of 16.6% in SNR was obtained. The calculations along with visual inspection revealed larger improvements in deeper regions, and the compounded image for the measured phantom showed a 3 mm diameter cyst not detectable in the reference image.

Compounding applied to SASB improves CNR and SNR results in images with a reduced speckle appearance. This was shown for simulations and confirmed on measured data.

I. Introduction

Ultrasound imaging is often used for many diagnostic purposes in clinical practice. Classifying e.g. a cyst as benign or malignant is dependent on high quality images having a high contrast and few artifacts. Synthetic Aperture Sequential Beamformation (SASB) is a method to construct B-mode images and was introduced by Kortbek et al [1] for a multi element linear array transducer. The technique showed a more range independent lateral resolution compared to Dynamic Receive Focusing (DRF) and reduced system complexity compared to full Synthetic Aperture systems. SASB consists of two seperate beamformers with the latter being the most complex. A single focal point in both transmit and receive are used in the first stage beamformer to construct scan lines in a similar way conventional systems uses Single Receive Focusing (SRF). In the second stage beamformer information from multiple first stage scan lines are combined to calculate each image point resulting in a high resolution image.

Ultrasound is subject to a number of artifacts e.g. speckle, which causes otherwise homogeneous regions to appear granular [2]. This reduces image contrast and makes identification and classification of cysts and tumors difficult. Recording images from several angles and combining these to a single image is the principle in spatial compounding [3]. Entrekin et al [4] has shown that compound imaging in conventional imaging systems significantly reduces speckle and reinforces real structures. This paper presents a novel implementation of SASB for compound imaging and studies the feasibility of applying spatial compounding using SASB for 2-dimensional medical imaging. The objective is to evaluate if the advantages of applying spatial compounding is obtained for improved image quality, compared to conventional SASB imaging. The method is evaluated on cyst phantoms using simulations and measurements.

II. Method

In SASB imaging data are recorded using a conventional sliding subaperture with a single focal point in transmit. To construct first stage scan lines a fixed receive time-delay profile is calculated from a receive focal point coincident with the transmit focal point. The focal point is considered as a virtual source and a number of virtual sources form a synthetic aperture used in the second stage beamformation. The result of the first stage beamformation is a real RF signal representing each scan line. Complex I/Q data samples are obtained from the sampled and demodulated RF signal for each first stage scan line. Data acquisition and first stage beamformation can be repeated for a number of different viewing angles M with individual angles given by $\theta_i, i = 1, ...M$.

The second stage beamformation produces a high resolution image consisting of numerous image points. The spatial position of the image points are independent of the viewing angle and to ease compounding they can preferable be placed on a rectangular grid as illustrated in Fig. 1. Multiple first stage scan lines contain information about each image point and the number of contributing lines increase with range. A single sample h, representing the image point at the location $\vec{r}_{ip}$ can

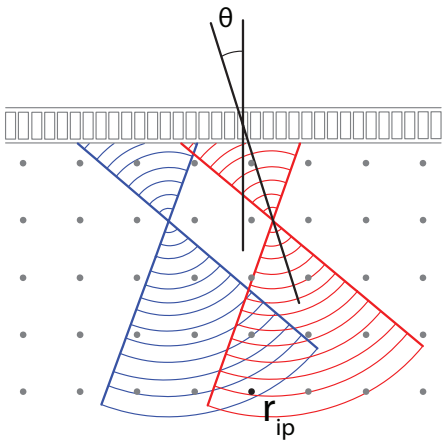

Fig. 1. Illustration of the propagating waves for two multi element emmisions (blue and red respectively) with beam direction θ. The black dot indicates a specific image point r_{ip} which is part of a rectangular grid placed independent of the viewing angle θ. The second stage image point contain information from two first stage scan lines used to calculate the sample value $h(r_{ip})$. The same rectangular grid is used for all viewing angles.

be expressed as

$$h(\vec{r}_{ip}) = \sum_{k=1}^{K(\vec{r}_{ip})} W(k, \vec{r}_{ip}) \cdot l_k(t_{d_k}(\vec{r}_{ip})) \tag{1}$$

where $l_k(t_{d_k}(\vec{r}_{ip}))$ is the I/Q sample from the contributing first stage line at time t_{d_k}, W is an apodization function and $K(\vec{r}_{ip})$ is the number of first stage scan lines containing information about the image point.
A complex valued second stage image point has the polar form representation

$$h(\vec{r}_{ip}) = a(\vec{r}_{ip}) \cdot e^{j\theta(\vec{r}_{ip})} \tag{2}$$

from which the amplitude can be found as $a(\vec{r}_{ip}) = |h(\vec{r}_{ip})|$. A sample in the compounded image h_c, at position $\vec{r}_{ip}$ is found by adding the amplitude $a(\vec{r}_{ip})$ for each steering angle

$$h_c(\vec{r}_{ip}) = \sum_{m=1}^{M} a_m(\vec{r}_{ip}) \tag{3}$$

where M denotes the number of different viewing angles.
The final B-mode image is constructed by logarithmically compressing data to a dynamic range of 60 dB followed by time gain compensation (TGC).
Contrast of the B-mode images are evaluated using contrast-to-noise ratio (CNR) based on a region of interest (ROI) and a background region (BR)

$$CNR = \frac{\mu_{ROI} - \mu_{BR}}{\sqrt{\sigma^2_{ROI} + \sigma^2_{BR}}} \tag{4}$$

where μ is the expectation value of the region and σ is its standard deviation.
Quantifying the amount of speckle, the speckle signal-to-noise ratio (SNR) is calculated as

$$SNR = \frac{\mu_{BR}}{\sigma_{BR}} \tag{5}$$

III. Results

The method is investigated using simulations of cyst phantoms, and measurements on a cyst phantom Model 571 (Danish Phantom Service, Frederikssund, Denmark) is used to validate the simulation results. B-mode images are created to extract quantitative information about CNR and SNR. The method is evaluated using a 192 element 7.5 MHz linear array transducer (BK Medical, Herlev, Denmark) with a 0.208 mm pitch. Using a 64 channel system 192 scan lines are acquired with transmit focus at 10 mm and F# = 2. The beamformation setup for SASB is specified in Table I.

TABLE I
BEAMFORMATION PARAMETERS

Parameter	Value
Virtual Source depth (mm)	10
Virtual Source F#	2
$\text{Apodization}_{\text{1st stage}}$ Tx / Rx	Boxcar / Gauss
$\text{Apodization}_{\text{2nd stage}}$	Hamming

A. Simulations

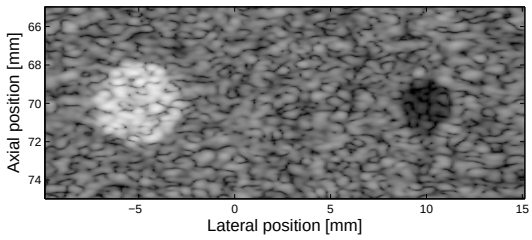

(a) Ordinary SASB

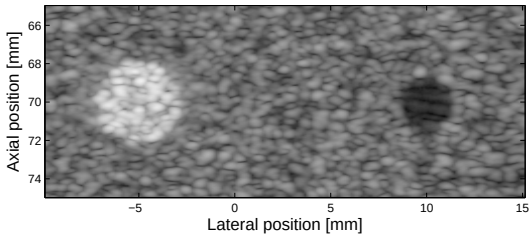

(b) Compound imaging using SASB

Fig. 2. Visualization of simulated echoic and anechoic cysts at 70 mm. A reference B-mode image using ordinary SASB (a) and compounded image with angles 0, ± 2 and ± 4 degrees (b) is shown.

Using the simulation software Field II [5], [6] data were acquired for five steering angles ($0, \pm 2, \pm 4$ degrees) using a cyst phantom containing echoic and anechoic cysts of different sizes at depths of 40, 50, 60, 70, and 80 mm. The beamformation is carried out using the Beamformation Toolbox III [7].
CNR and SNR are calculated for B-mode images with 60 dB

dynamic range. Comparing the white cyst in Fig. 2(a) and 2(b) show an improvement in CNR of 26.9% using compounding, whereas CNR for the black cyst is improved by 56.6%. At 70 mm SNR shows an improvement by 10.8%.

Calculating CNR for all the simulated cysts yield on average an improvement of 33.2% compared to the values obtained from the reference image. For regions of increasing depth SNR was on average increased by 9.3%.

To further illustrate the improvements introduced by compounding a cross section with the amplitudes of the image values in Fig. 2(a) and 2(b) is obtained. The cross section is made at 70 mm expanding laterally over the images and are shown in Fig. 3(a) and 3(b). The plot corresponding to the compounded image shows smaller variations compared to the reference image and this results in an improvement in SNR as calculated. The positive peak centered around -5 mm corresponds to the echoic cyst whereas the negative peak centered around 10 mm corresponds to the anechoic cyst. It is observed that the outline of the cysts are more defined in Fig. 2(b).

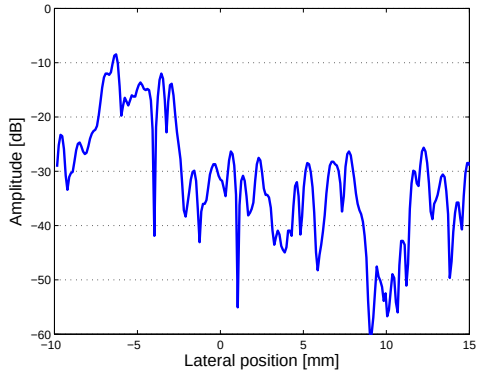

(a) Ordinary SASB

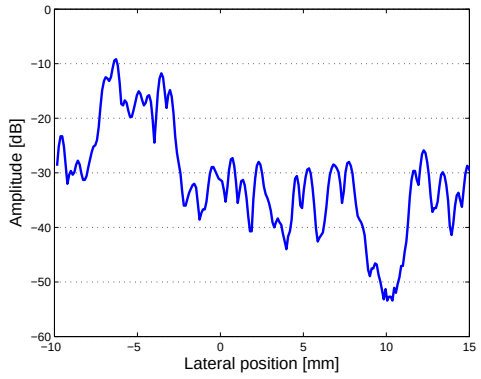

(b) Compound imaging using SASB

Fig. 3. Overview of the amplitude values at 70 mm expanding laterally over the B-mode images in Fig. 2(a) and 2(b).

B. Measurements

The simulation results are validated through measurements using a ProFocus scanner (BK Medical, Herlev, Denmark) equipped with a research interface for acquisition of beamformed RF data described in [8], [9]. Transmit- and receive delay profile, apodization, and excitation waveform are preset standardized settings from the manufacturer. SASB first stage RF data were acquired and subsequently processed off-line using the Beamformation Toolbox III to generate the final second stage data. Measurements are performed using five different beam directions $(0, \pm 2, \pm 4$ degrees).

B-mode images based on measurement on the cyst phantom are shown for the reference in Fig. 4(a) and for the compounded in Fig. 4(b). The CNR and SNR are calculated using

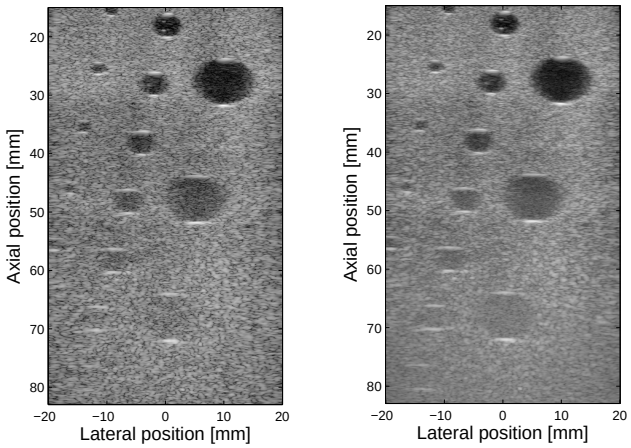

(a) Ordinary SASB (b) Compound imaging using SASB

Fig. 4. Visualization of measurement on cyst phantom, using (a) ordinary SASB (b) compounding using five angles.

(4) and (5). CNR of cysts at depths from 18 to 78 mm with a separation of 10 mm are on average improved by 45.9%. On average an improvement of 16.6% in SNR for regions of increasing depth is obtained. The calculations along with visual inspection reveal larger improvements in deeper regions, and the compounded image for the measured phantom shows a 3 mm diameter cyst not detectable in the reference image.

For a better appreciation of the reduction in speckle appearance Fig. 5(a) and 5(b) shows zoomed images of cysts at depth of 48 mm. Looking at the background region in Fig. 5(b) reveals a less prominent speckle pattern compared to Fig. 5(a). Due to the nature of water cysts no speckle is expected inside the perimeter of the cysts. The fluctuation inside the cysts in Fig. 5(a) are caused by noise and this noise is reduced in the compounded image resulting in better CNR values.

Investigating the effect of an increasing number of angles used for compounding, CNR and SNR values are calculated for images using respectively 1, 3 and 5 angles with an angular seperation of 2 degrees. The results of CNR are showed in Fig. 6(a) and for SNR in Fig. 6(b), and for an increasing number of images CNR and SNR values are increasing at all the depths. Note that the SNR values are higher in deeper regions of the images due to blurring effects.

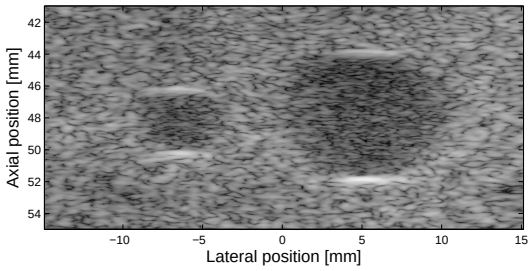

(a) Ordinary SASB

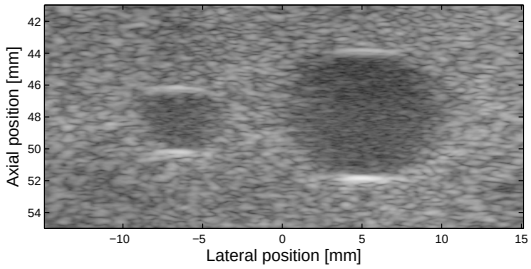

(b) Compound imaging using SASB

Fig. 5. Visualization of measured water cysts at depth of 48 mm. A reference B-mode image using ordinary SASB (a) and compounded image with angles 0, ± 2 and ± 4 degrees (b) is shown.

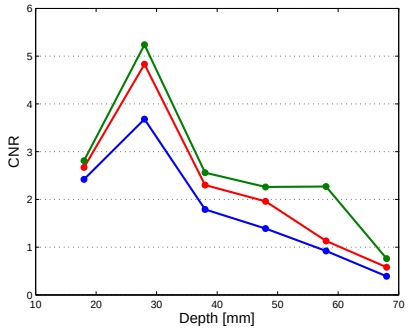

(a) CNR

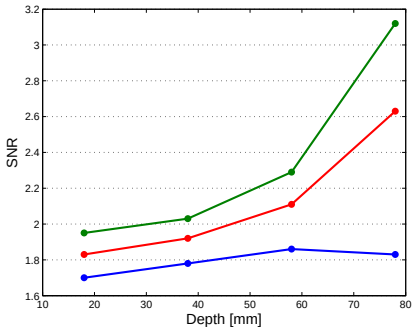

(b) SNR

Fig. 6. CNR values (a) and SNR values (b) at increasing depth computed from SASB images using 1 (blue), 3 (red) and 5 (green) images for compounding.

IV. Conclusions

Spatial compounding using SASB images has been succesfully implemented for a linear multi element array transducer. Compounding of a number of images is based on SASB second stage image points positioned on a rectangular grid independent of individual beam directions. The effect of compounding is evaluated on an ordinary SASB image and compounding of five images recorded for steering angles $0, \pm 2, \pm 4$ degrees. Results obtained from simulated cysts show improvements in CNR and SNR which on average is improved by 33.2% and 9.3% respectively. Measurements on a cyst phantom confirmed the results from the simulation. CNR shows an improvement by 45.9% on average while SNR is improved by 16.6% on average. Results from Fig. 6(a) and 6(b) show higher contrast and less speckle using 5 angles for compounding compared to using 3 and 1 angle.

The method results in reduced speckle appearence in B-mode images and a reduced level of noise especially evident in anechoic cysts. As a consequence, the contrast is improved making classification of cysts and other structures easier.

Implementing compounding using SASB on data acquired with a convex array transducer, and *in-vivo* studies are suggestions for further investigations.

Acknowledgement

This work was supported by BK Medical ApS, Denmark, by providing an ultrasound scanner making data recording possible.

References

[1] J. Kortbek, J. A. Jensen, and K. L. Gammelmark, "Synthetic aperture sequential beamforming," in *Proc. IEEE Ultrason. Symp.*, 2008, pp. 966–969.

[2] C. Burckhardt, "Speckle in ultrasound b-mode scans," *IEEE Trans. Son. Ultrason.*, vol. SU-25, no. 1, pp. 1–6, Jan. 1978.

[3] S. K. Jespersen, J. E. Wilhjelm, and H. Sillesen, "Multi-angle compound imaging," *Ultrason. Imaging*, vol. 20, pp. 81–102, 1998.

[4] R. Entrekin, P. Jackson, and B. Porter, "Real time spatial compound imaging in breast ultrasound: technology and early clinical experience," *medicamundi*, vol. 43, pp. 35–43, September 1999.

[5] J. A. Jensen, "Field: A Program for Simulating Ultrasound Systems," *Med. Biol. Eng. Comp.*, vol. 10th Nordic-Baltic Conference on Biomedical Imaging, Vol. 4, Supplement 1, Part 1, pp. 351–353, 1996.

[6] J. A. Jensen and N. B. Svendsen, "Calculation of Pressure Fields from Arbitrarily Shaped, Apodized, and Excited Ultrasound Transducers," *IEEE Trans. Ultrason., Ferroelec., Freq. Contr.*, vol. 39, pp. 262–267, 1992.

[7] J. M. Hansen, M. C. Hemmsen, and J. A. Jensen, "An object-oriented multi-threaded software beam formation toolbox," in *Proc. SPIE - Medical Imaging - Ultrasonic Imaging and Signal Processsing*, vol. 7968, 2011, pp. 79 680Y–9.

[8] M. C. Hemmsen, M. M. Petersen, S. I. Nikolov, M. B. Nielsen, and J. A. Jensen, "Ultrasound image quality assessment: A framework for evaluation of clinical image quality," in *SPIE Med. Imag. V Symp.*, vol. 76291, 2010, pp. 76 290C–12.

[9] M. C. Hemmsen, S. I. Nikolov, M. M. Pedersen, M. J. Pihl, M. S. Enevoldsen, J. M. Hansen, and J. A. Jensen, "Implementation of a versatile research data acquisition system using a commercially available medical ultrasound scanner," *IEEE Trans. Ultrason., Ferroelec., Freq. Contr.*, p. Accepted for publication, 2011.